DIAGNOSTICS OF A SIMULATED FLUX TUBE EMERGENCE

Lotfi Yelles Chaouche, Mark Cheung, Andreas Lagg, and Sami Solanki

Max-Planck-Institut für Sonnensystemforshung, 37191 Katlenburg-Lindau, Germany

ABSTRACT

We have carried out spectro-polarimetric diagnostics of a 3-D radiation MHD simulation of an emerging flux tube in the solar photosphere. We consider a time sequence starting from the appearance of the flux tube at the solar surface and follow it until it reaches the top of the photosphere. The Stokes profiles of two iron lines (630.1 nm and 630.2 nm) are calculated. Using an inversion based on the Milne-Eddington approximation, we determine physical quantities from the Stokes profiles and compare them with their original values in the simulation. This will facilitate the interpretation of observational results.

Key words: Sun; flux emergence; magnetic fields.

1. INTRODUCTION

Observations of emerging flux regions have been reported several times in the literature (Brants 1985; Lites et al. 1998; Sigwarth 2000). On the other hand the computer facilities available today make it feasible to carry out 3-D realistic radiative magneto-convection simulations (Vögler et al. 2005). We have carried out spectro-polarimetric diagnostics of a simulated flux tube emergence in the photosphere in order to make comparison with observations. This link between simulation and observations can help to better understand the emergence process and also to improve the numerical simulations.

2. SIMULATION OF AN EMERGING FLUX TUBE

The simulation of an emerging flux tube was carried out using a compressible 3D radiation MHD code (MURaM) (Vögler et al. 2005), which solves the MHD equations taking into account energy exchange via radiative transfer as well as the effect of partial ionization in the equation of state.

The horizontal size of the simulation domain is 24 × 12 Mm, spanned by 480 and 240 grid-points respectively. The height of the domain is 2.3 Mm, and is spanned by 144 grid-points. The resulting grid-spacing in the horizontal and vertical directions is 50 and 16 km respectively. The vertical side boundaries are periodic. Both the bottom and top boundaries are open and allow mass transfer. The top boundary is at about 500 km above the surface of the sun $\tau = 1$.

At $t = 0$, a horizontal, axisymmetric flux tube was introduced 1.5 Mm below the visible surface. The initial longitudinal and transverse components of the magnetic field are given by:

$$B_l(r) = B_0 \exp\left(-r^2/R_0^2\right), \quad (1)$$

$$B_\theta(r) = \frac{\lambda r}{R_0} B_l, \quad (2)$$

for $r \in [0, 2R_0]$, where r is the radial distance from the tube axis. $R_0 = 200$ km is the characteristic radius of the tube and $B_0 = 8500$ G is the magnetic field strength at the tube axis. The parameter $\lambda = 0.5$ specifies the amount of twist in the tube. The plasma-β (ratio between gas and magnetic pressures, both taken inside the tube) is approximately equal to 1 at the center of the tube. The initial longitudinal flux of the tube is $\Phi_0 = 10^{19}$ Mx. The flux tube has uniform specific entropy equal to the average value of the surrounding upflows.

Figure 1 shows the maps of the continuum intensity at three different times. The left panel ($t = 7.7$ min) shows the intensity at an early stage of the emergence. At this time, parts of the flux tube are just beginning to transverse the visible surface. The middle and right panels show the field of view at t=11.3 min and $t = 16.1$ min respectively. At these times, the flux tube is still relatively coherent. At later stages (not shown here) the convection distorts the magnetic flux tube, and the magnetic field is more concentrated in the intergranular lanes.

3. SYNTHETIC LINE PROFILES

Using the STOPRO code (Solanki 1987; Frutiger et al. 2000), we synthesized the full set of Stokes profiles for the emergence simulation. Profiles for the iron FeI lines 630.1 nm and 630.2 nm lines were synthesized under the assumption of local thermodynamic equilibrium (LTE). For different snapshots of the simulation, synthetic line

Proceedings of the 11th European Solar Physics Meeting - The Dynamic Sun: Challenges for Theory and Observations, 11-16 September 2005 (ESA SP-596, December 2005)

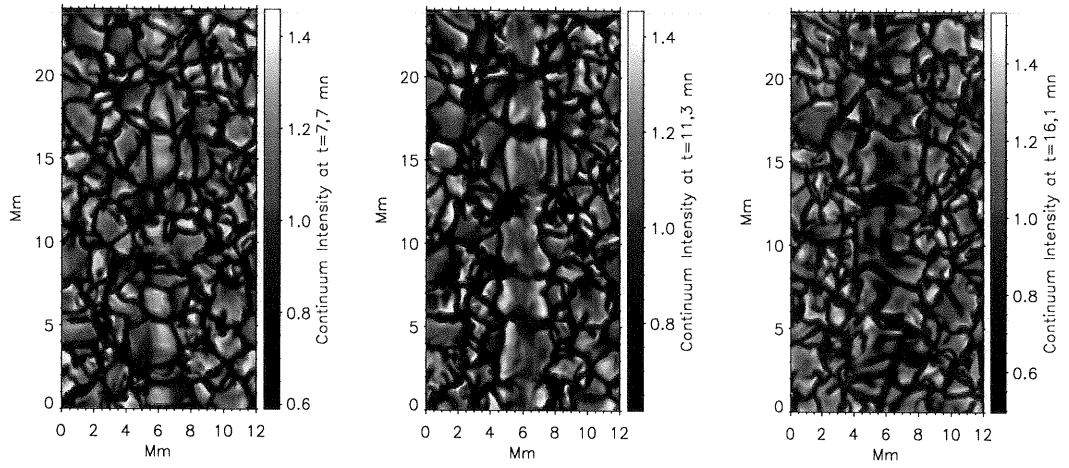

Figure 1. Maps of the continuum intensity near the $630.2nm$ *line at three different times. From left to right* $t = 7.7$ *min,* $t = 11.3$ *min and* $t = 16.1$ *min.*

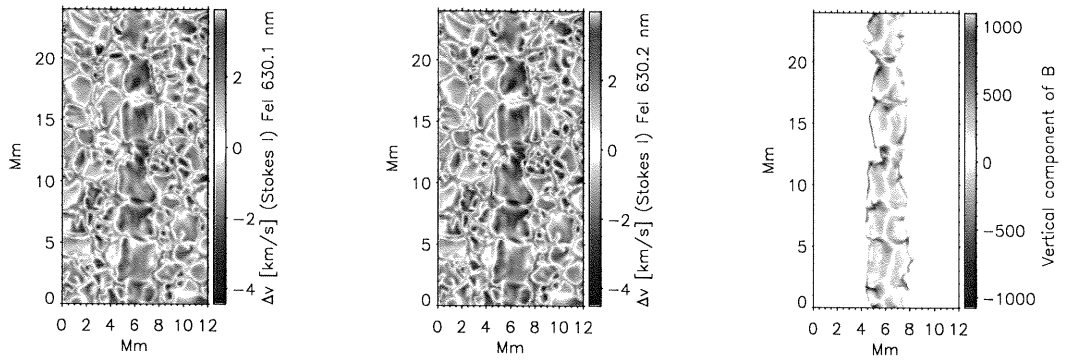

Figure 2. Vertical velocity determined from doppler shifts of Stokes-I in 630.1 *nm and* 630.2 *nm lines (left and middle panels respectively); and strength of the vertical component of the magnetic field (right panel) calculated from Stokes-I and Stokes-V at* $t = 11.3$ *min.*

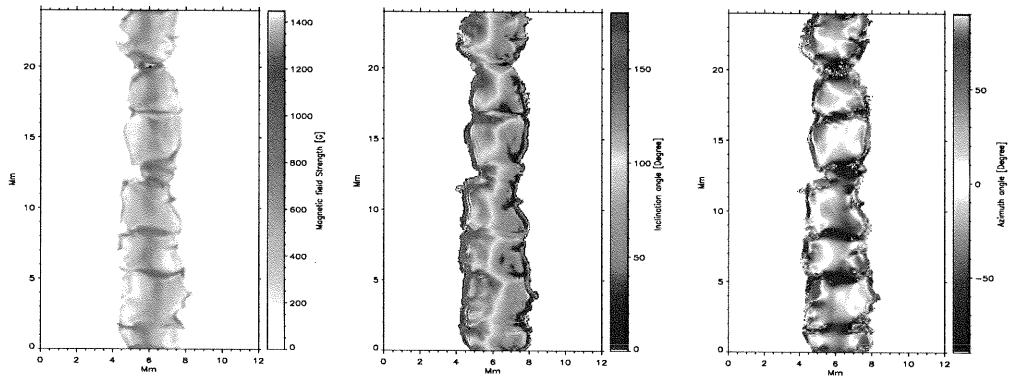

Figure 3. Vector magnetic field from an inversion of the Stokes parameters of 630.2 line.

profiles were calculated over the entire simulation domain.

Figure 2 shows a snapshot of the simulation at $t = 11.3$ min, as revealed by the Stokes analysis. The left and middle panels show the synthetic 'Dopplergrams' (left and middle panels) as determined from the Doppler shifts of the two FeI lines (see Equations (3) and (4)). A negative velocity corresponds to upwards moving material. The measurement of the Doppler shift of the two lines yield almost identical distributions of the Doppler velocity. There is a clear signature in the Doppler velocity that shows the emerging flux tube. At this early phase of emergence, the flux tube is still relatively coherent.

The doppler shift is given by :

$$\Delta v = c(\lambda_0 - \lambda_c)/\lambda_0 \tag{3}$$

and λ_c is the center of gravity of the line :

$$\lambda_c = \frac{\int [I_c - I(\lambda)]\lambda d\lambda}{\int [I_c - I(\lambda)] d\lambda} \tag{4}$$

where c is the speed of light, λ_0 is the wavelength of the line center in the rest frame. I_c is the continuum intensity and $I(\lambda)$ is the Stokes-I profile.

The right panel of Figure 2 shows a synthetic 'magnetogram' (B_z) at $t = 11.3$ min as calculated from Stokes-V and I with the center of gravity technique (Semel 1985) . The left and right halves of the tube have opposite polarities because of the tube's twist.

The contribution function of these two iron lines has a maximum near optical depth $\tau = 0.1$. This means that the Doppler velocities and the magnetic strengths as shown in Figure 2 most closely corresponds to the values of these quantities at that height in the atmosphere. In the following section we extend our analysis of the synthetic Stokes profiles by processing them with an inversion code.

4. INVERSION OF THE STOKES PROFILES

In order to retrieve the atmospheric conditions in which these two iron lines formed, we carried out an inversion of their Stokes profiles. The advantage here is that we already know the values of the physical quantities in-situ from the numerical simulations. Thus we can compare the results from the inversion with the in-situ values at the appropriate optical depth.

As example for the inversion Figure 3 shows the vector magnetic field $\vec{B}$ at $t = 11.3$ min. The left panel shows the magnetic field strength. The central panel shows the inclination angle of $\vec{B}$. An inclination of 0° degrees means that the vector is anti-parallel to the line-of-sight and an inclination of 90° means the field is horizontal. The right panel shows the azimuthal angle, with zero degrees indicating a direction perpendicular to the tube axis. The inversion was carried out using a Milne-Eddington atmosphere with the "$Linefit$" code (Lagg et al. 2004).

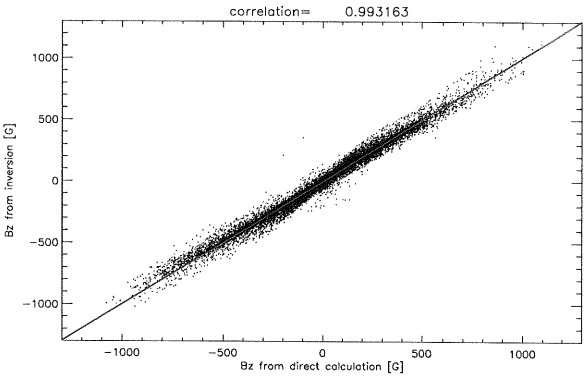

Figure 4. Scatterplot of the vertical component of the magnetic field obtained from the center of gravity technique and from inversion of 630.2 *nm line.*

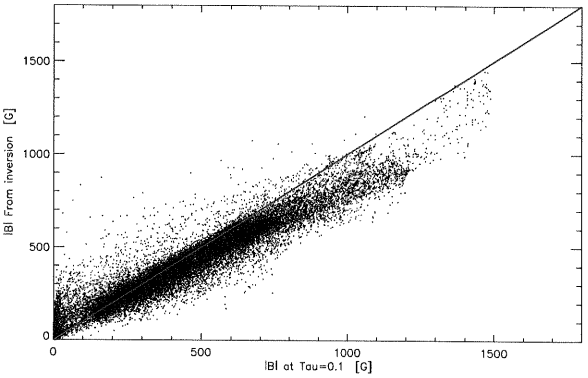

Figure 5. Scatterplot of the strength of the magnetic field at $\tau = 0.1$ *and the one from inversion of* 630.2 *nm line.*

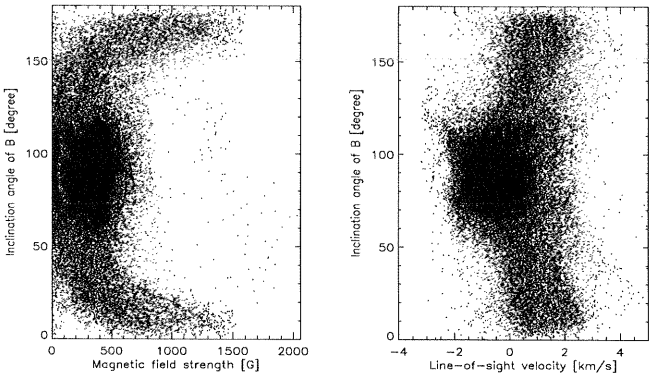

Figure 6. Scatter plots of the Magnetic field strength and Line-of-sight velocity versus the inclination angle of the magnetic field.

Figure 4 shows the comparison between the value of B_z as obtained using the center-of-gravity technique (see § 3) and the values obtained from the Milne-Eddington inversion. In this plot, both sets of values were calculated for the snapshot at $t = 11.3$ min. There is a very good agreement between the values as obtained from these two methods. We have repeated the comparison for other snapshots of the simulation and the match in those cases is also good.

In Figure 5 we compare the strength of the magnetic field from the inversion with the one from MHD simulation at $\tau = 0.1$ and $t = 11.3$ min. We chose this optical depth since the contribution functions have their maximum close to this level for most of the simulation domain. We notice that the correlation is better for average field strength between 200 G and 700 G. There is less correlation when the field is above 800 G and below 100 G. In the case of magnetic field above 800 G the line is formed with more contribution from higher atmospheric layers (where the magnetic field is weaker). For the magnetic fields below 100 G the line get more contribution from below. In this latter case the non-correlation can also be due to the fact that the uncertainties associated with the inversion procedure is larger for weak fields.

5. COMPARISON WITH OBSERVATIONS

Figure 6 shows two scatter plots of quantities as obtained from the inversion. The left panel shows a scatter plot of the inclination angle of $\vec{B}$ versus the absolute field strength. The right panel shows the inclination of $\vec{B}$ versus the line-of-sight (vertical) velocity. Both have been calculated for time $t = 16.1$ min. At this later stage of the simulation, some of the emerged magnetic flux has already been swept into the intergranular lanes. These regions are mostly vertical and have kilogauss field strengths. The horizontal field, on the other hand, have sub-kilogauss field strengths. This behaviour has also been reported in observations of emerging flux regions (Lites et al. 1998).

A more realistic comparison between simulated data and observations can be done by smoothing the Stokes profiles obtained from simulations. Thus a convolution of the Stokes parameters with a Point Spread Function (PSF) taking into account the effect of finite resolution of the telescope and the atmospheric dispersion is needed. This work is now in process.

REFERENCES

Brants, J. J. 1985, Solar Phys., 95, 15

Frutiger, C., Solanki, S. K., Fligge, M., & Bruls, J. H. M. J. 2000, Astron. & Astrophys., 358, 1109

Lagg, A., Woch, J., Krupp, N., & Solanki, S. K. 2004, Astron. & Astrophys., 414, 1109

Lites, B. W., Skumanich, A., & Martinez Pillet, V. 1998, Astron. & Astrophys., 333, 1053

Semel, M. 1985, LNP Vol. 233: High Resolution in Solar Physics, 233, 178

Sigwarth, M. 2000, Reviews of Modern Astronomy, 13, 45

Solanki, S. K. 1987, Ph.D. Thesis

Vögler, A., Shelyag, S., Schüssler, M., et al. 2005, Astron. & Astrophys., 429, 335